35th EPS Conference on Plasma Phys. Hersonissos, 9 - 13 June 2008 ECA Vol.**32D**, P-5.021 (2008)

Poloidal drift of trapped particle orbits in real-space coordinates *

V. V. Nemov[1,2], S. V. Kasilov[1,2], W. Kernbichler[2], G. O. Leitold[2]

[1]*Institute of Plasma Physics, National Science Center "Kharkov Institute of Physics and Technology", Ukraine*

[2]*Association EURATOM-ÖAW, Institut für Theoretische Physik - Computational Physics, TU Graz, Austria*

Introduction

The bounce averaged poloidal drift velocity of trapped particles in stellarators is an important quantity in the framework of optimization of stellarators because it allows to analyze the possibility for closure of contours of the second adiabatic invariant and therefore for improvement of α-particle confinement in such a device (see, e.g., [1]). In this report, a method is presented to compute such a drift velocity directly in real space coordinates through integration along magnetic field lines. This has the advantage that one is not limited to the usage of magnetic coordinates and can use the magnetic field produced by coil currents and more importantly also results of three-dimensional MHD finite beta equilibrium codes such as PIES [2] and HINT [3].

Basic equations

A Clebsch representation of the magnetic field $\mathbf{B}$, $\mathbf{B} = \nabla\psi \times \nabla\theta_0$, is used where ψ labels a regular or island magnetic surface and θ_0 labels a given field line on a magnetic surface. As the third coordinate φ is taken which is counted along the magnetic field line. The equations for particle motion (3.41) of Ref. 4 are used. In $(\psi, \theta_0, \varphi)$ notation these equations are given as

$$\frac{d\psi}{dt} = \frac{cv_\parallel}{eB\sqrt{g}}\left[\frac{\partial}{\partial\theta_0}(mv_\parallel h_\varphi) - \frac{\partial}{\partial\varphi}(mv_\parallel h_{\theta_0})\right], \quad (1)$$

$$\frac{d\theta_0}{dt} = \frac{cv_\parallel}{eB\sqrt{g}}\left[\frac{\partial}{\partial\varphi}(mv_\parallel h_\psi) - \frac{\partial}{\partial\psi}(mv_\parallel h_\varphi)\right], \quad (2)$$

$$\frac{d\varphi}{dt} \approx v_\parallel h^\varphi, \quad (3)$$

where $v_\parallel = \sigma\sqrt{v^2 - J_\perp B}$, $v^2 = 2(w - e\Phi)/m$, $J_\perp = v_\perp^2/B$, $\sigma = \pm 1$, $\sqrt{g}$=$1/(\nabla\psi \times \nabla\theta_0 \cdot \nabla\varphi)$, $h^\psi = h^{\theta_0} = 0$, $h^\varphi = 1/(B\sqrt{g})$, h^ψ, h^{θ_0} and h^φ are the contravariant components of the unit vector $\mathbf{h} = \mathbf{B}/B$, h_ψ, h_{θ_0} and h_φ are the covariant components of this vector. The poloidal motion of trapped particles is characterized by the increment of θ_0, $\Delta\theta_0$, during one bounce period. In general, in toroidal geometry $\nabla\theta_0$ is not single valued. This makes problems in simultaneous calculations for a variety of trapped particles distributed along the magnetic field line. To avoid these problems, a further transition is performed from θ_0 to a variable θ connected with θ_0 by

$$\theta = \theta_0 + \chi\varphi, \quad (4)$$

with χ=$\chi(\psi)$ and $\nabla\theta$ being single valued quantities. From (4) χ' can be found as

$$\chi' = -\lim_{\varphi\to\infty}\frac{1}{\varphi}\frac{\nabla\theta_0 \cdot \nabla\psi}{|\nabla\psi|^2}, \quad (5)$$

*This work, supported by the European Communities under the contract of Association between EURATOM and the Austrian Academy of Sciences, was carried out within the framework of the European Fusion Development Agreement. The views and opinions expressed herein do not necessarily reflect those of the European Commission. Additional funding is provided by the Austrian Science Foundation, FWF, under contract number P16797-N08.

where prime denotes the derivative with respect to ψ. For a magnetic field given in real-space coordinates the computation of $\nabla\psi$ using integration along the field lines has been formerly discussed (e.g., in [5]). The computation of $\nabla\theta_0$ can be performed using the same equations as for $\nabla\psi$ but a starting value for $\nabla\theta_0$ should be different from the starting value for $\nabla\psi$ [$\nabla\theta_{0st} = (\mathbf{B}\times\nabla\psi_{st})/|\nabla\psi_{st}|^2$, according to the Clebsch representation of $\mathbf{B}$].
From the relation between θ and θ_0 (4) one can derive

$$\frac{d\theta}{dt} = \frac{d\theta_0}{dt} + \chi\frac{d\varphi}{dt} + \varphi\chi'\frac{d\psi}{dt}\ . \tag{6}$$

Substituting (1)-(3) into (6) and integrating with respect to t for one bounce period, τ_b, one finds

$$\Delta\hat{\theta} = -\frac{c}{e}\oint\left[\frac{\partial}{\partial\psi}(mv_\parallel h_\varphi) - \varphi\chi'\frac{\partial}{\partial\theta_0}(mv_\parallel h_\varphi)\right]d\varphi + \chi'\frac{c}{e}\oint mv_\parallel h_{\theta_0}d\varphi\ . \tag{7}$$

After a series of transformations and dividing $\Delta\hat{\theta}$ by τ_b to define $d\theta/dt$ one obtains

$$\hat{v}_{\theta,i} = |\mathbf{e}_{\theta_0,i}|\frac{d\theta}{dt},\quad \frac{d\theta}{dt} = \frac{v^2B_0}{2\omega_{c0}}\left[\frac{\partial\hat{G}_j/\partial b'}{\partial\hat{I}_j/\partial b'} + \frac{2}{3}\frac{\partial\hat{V}_j/\partial b'}{\partial\hat{I}_j/\partial b'} + \frac{2e}{mv^2}\,\Phi'\right], \tag{8}$$

where $\hat{v}_{\theta,i}$ is the velocity of the bounce averaged poloidal drift $\mathbf{e}_{\theta_0} = \sqrt{g}(\nabla\varphi\times\nabla\psi)$, $\omega_{c0} = eB_0/(mc)$, b' is the pitch-angle variable connected with $J_\perp$ as $b' = v^2/(J_\perp B_0)$, B_0 is some reference magnetic field. The quantities $\hat{G}_j$, $\hat{V}_j$ and $\hat{I}_j$ are determined as

$$\hat{G}_j = \frac{1}{3}\int_{s_j^{min}}^{s_j^{max}}\frac{\mathrm{d}s}{B}\sqrt{1-\frac{B}{B_0b'}}\left(4\frac{B_0}{B}-\frac{1}{b'}\right)\frac{1}{B_0}\frac{\partial B}{\partial\psi},\ \hat{I}_j = \int_{s_j^{min}}^{s_j^{max}}\frac{\mathrm{d}s}{B}\sqrt{1-\frac{B}{B_0b'}}\,, \tag{9}$$

$$\hat{V}_j = \int_{s_j^{min}}^{s_j^{max}}\frac{\mathrm{d}s}{B^2}\left(1-\frac{B}{B_0b'}\right)^{3/2}\left[\chi'(\nabla\psi\times\mathbf{h})\cdot\nabla\varphi - \left(2\frac{\partial B}{\partial\psi} - \frac{B}{B^\varphi}\frac{\partial B^\varphi}{\partial\psi}\right)\right], \tag{10}$$

$$\frac{\partial B}{\partial\psi} = \frac{1}{B^\varphi}\nabla B\times(\nabla\theta_0+\chi'\varphi\nabla\psi)\cdot\nabla\varphi,\ \frac{\partial B^\varphi}{\partial\psi} = \frac{1}{B^\varphi}\nabla B^\varphi\times(\nabla\theta_0+\chi'\varphi\nabla\psi)\cdot\nabla\varphi, \tag{11}$$

where B^φ=$\mathbf{B}\cdot\nabla\varphi$, $\nabla\theta_0+\chi'\varphi\nabla\psi$ is a single valued quantity in the case of χ' defined by (5), s is the length along the magnetic field line. The index j numbers the s intervals [s_j^{min}, s_j^{max}] where $b'-B/B_0\geq 0$, whereas the index i in (8) numbers local minima of B along s.

Computational results

Using a field line tracing code Eqs. (8)-(11) are solved in cylindrical coordinates (ρ,φ,z) for some magnetic surfaces of the CHS [6] standard and the drift-orbit optimized (inward shifted) configurations and W7-X. Computations of $\mathbf{B}$ are performed using the Biot-Savart law code (for CHS) or data from the HINT2 code (for W7-X equilibrium with finite β) as in Refs. [7,8] where studies of the effective ripple for CHS and W7-X have been carried out.
Figures 1 - 3 show results for CHS by one appropriate magnetic surface for every configuration. The mean radius of the magnetic surface is indicated on the plots. Fig. 1 illustrates the behavior of $\nabla\theta_0\cdot\nabla\psi/(\varphi|\nabla\psi|^2)$ [see Eq. (5)] along the magnetic field line for the magnetic surface of the CHS standard configuration. It can be clearly seen how this quantity approaches the final value of χ'. Once χ' has been computed $\hat{v}_\theta$ can be calculated with the help of Eqs. (8)-(11). Fig. 2 (middle) shows corresponding to Fig. 1 characteristic results of such calculations in a normalized form $v_{\theta,norm}$ as functions of the pitch $\gamma = v_{\parallel 0}/v_{\perp 0}$, where $v_{\parallel 0}$ is $v_\parallel$ at a local minimum of B and $v_{\perp 0} = \sqrt{J_\perp B_0}$. The curves are marked in accordance with the numbers of the

minima of B in the distribution of B/B_0 along the magnetic field line which is shown at the top of Fig. 2. Also, at the bottom, the angle $\gamma_{J_\parallel}$ between the $J_\parallel$ contour and the magnetic surface cross-section is shown in a normalized form γ_c

$$\gamma_c = \frac{2}{\pi}\gamma_{J_\parallel} \ , \ \ \gamma_{J_\parallel} = \arctan\frac{v_{\mathrm{an},i}}{\hat{v}_{\theta,i}} \ , \tag{12}$$

where $v_{\mathrm{an},i}$ is the velocity of the radial bounce-averaged trapped particle drift which can be calculated using the corresponding equations of [5]. In the calculations, $|\gamma_c|$ can be realized within the limits $[0,1]$. For $|\gamma_c| = 1$ the $J_\parallel$ contour is perpendicular to the magnetic surface and most probably such a contour is not closed. For small $|\gamma_c|$ the angle between the $J_\parallel$ contour and the magnetic surface is small and one can expect that the corresponding $J_\parallel$ contour is closed and is closely tied to the magnetic surface. Analogous results for the drift-orbit-optimized CHS configuration are shown in Fig. 3 where the distribution of B/B_0 along the magnetic field line shows the characteristic look of σ-optimization (full σ-optimization would mean that all minima have exactly the same value). One can also see that the fraction of trapped particles with v_θ values close to zero (and $|\gamma_c|$ close to unity) is much smaller than that for the standard configuration which is a clear result of the optimization. Additional results including those for W7-X have been presented in Ref. [9].

Summary

The obtained equations have been solved in real space coordinates using a field line tracing code for the magnetic field computed using the Biot-Savart law code (for CHS) or data from the HINT2 code (for W7-X equilibrium with finite β). Combining studies of the radial drift as well as the poloidal drift one can conveniently assess the character of $J_\parallel$ contours in the neighborhood of a magnetic surface. Small values of the parameter γ_c [Eq. (12)] indicate poloidally closed contours of $J_\parallel$ which are closely tied to the magnetic surface whereas $|\gamma_c|$ values close to unity definitely indicate the presence of unclosed contours of $J_\parallel$. To illustrate the approach, computations for two stellarator configurations with quite different results have been shown. For the inward shifted CHS configuration, one can see the beneficial effect of σ-optimization on the bounce averaged poloidal drift velocity and the pertinent closure of contours of $J_\parallel$. The results for W7-X are in a reasonable correlation with the results obtained formerly in magnetic coordinates. The presented approach very well complements the effective ripple as target quantity for optimization by putting more significance to fast particle confinement which is not covered well by the effective ripple.

References

[1] M. I. Mikhailov, V. D. Shafranov, A. A. Subbotin, et al., Nucl. Fusion **42**, L23 (2002).

[2] A. H. Reiman and H. S. Greenside, J. Comput. Phys. **75**, 423 (1988).

[3] Y. Suzuki, N. Nakajima, K. Watanabe, et al., Nucl. Fusion **46**, L19 (2006).

[4] A. I. Morozov and L. S. Solov'ev, in *Reviews of Plasma Physics*, edited by M. A. Leontovich (Consultants Bureau, New York, 1966), Vol. 2, p. 201

[5] V. V. Nemov, S. V. Kasilov, W. Kernbichler and M. F. Heyn, Phys. Plasmas **6**, 4622 (1999).

[6] S. Okamura, K. Matsuoka, R. Akiyama, et al., Nucl . Fusion **39**, 1337 (1999).

[7] M. F. Heyn et al., *Plasma Phys. Control. Fusion*, **43**, 1311 (2001).

[8] V. V. Nemov et al., in *34th EPS Conference on Plasma Physics, Warsaw, Poland, 2-6 July 2007*, ECA Vol. **31F**, P-4.063.

[9] V. V. Nemov, S. V. Kasilov, W. Kernbichler and G. O. Leitold, Phys. Plasmas **15**, 052501 (2008).

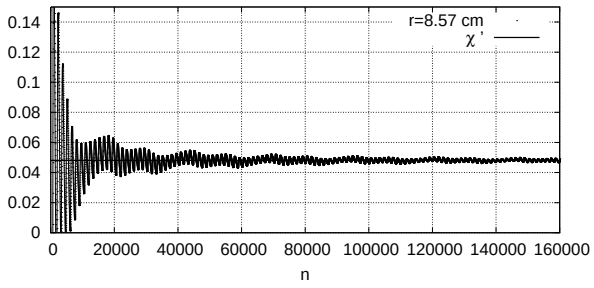

Fig.1. Determination of χ' for the standard configuration of CHS for a magnetic surface with a moderate distance from the magnetic axis; n is the number of integration steps along the field line with 1280 steps per magnetic field period.

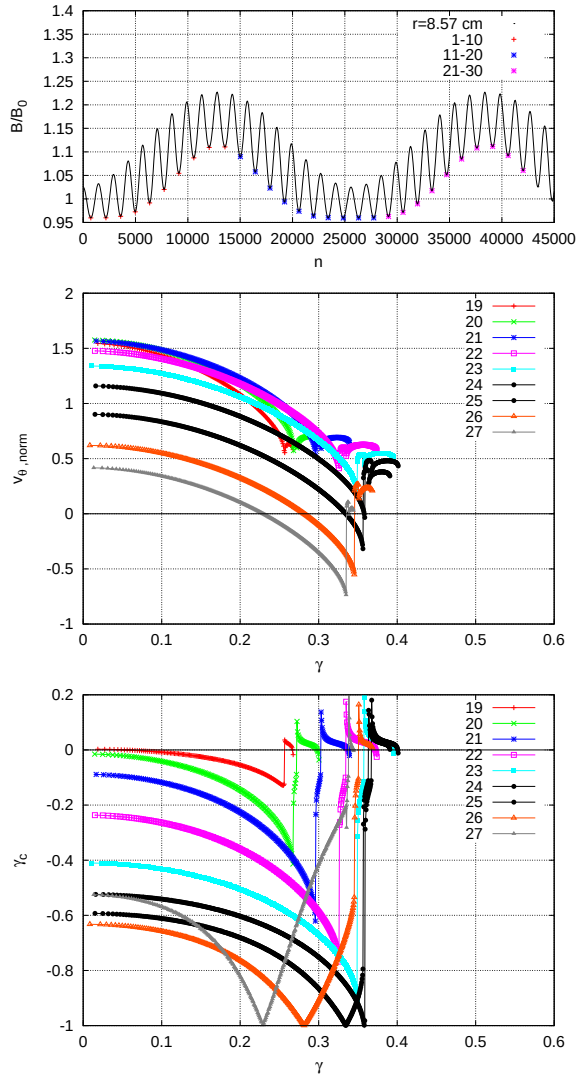

Fig.2. Computational results for a magnetic surface of the standard CHS configuration: (top) distribution of B/B_0 along the magnetic field line (n is the same as in Fig. 1); (middle) $v_{\theta,norm}$ as a function of pitch-angle γ for local minima of B as indicated in the Figure; (bottom) parameter γ_c as a function of γ for the same local minima of B.

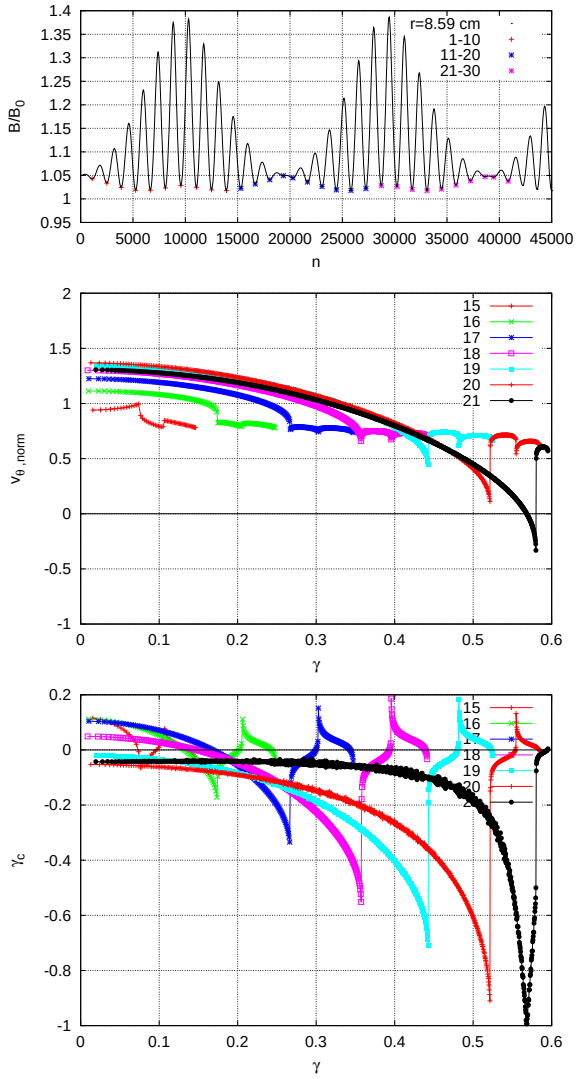

Fig.3. Same as Figure 2 for a magnetic surface of the drift-orbit optimized CHS configuration.